Performance of a Large Scale Scintillating Fiber Tracker Using VLPC Readout

D. Adams[h], M. Adams[b], B. Baumbaugh[f], I. Bertram[h], A. Bross[a], D. Casey[i], S. Chang[e], M. Chung[b], C. Cooper[g], R. Demina[e], G. Fanourakis[i], T. Ferbel[i], S. Grünendahl[i], J. Hinson[g], B. Howell[g], H. Johari[e], J. S. Kang[c], C. L. Kim[c], S. K. Kim[j], D. Koltick[g], F. Lobkowicz[i], S. Margulies[b], J. Moromisato[e], M. Narain[a], C. H. Park[a], Y. M. Park[d], S. Reucroft[e], R. Ruchti[f], J. Solomon[b], E. VonGoeler[e], J. Warchol[f], M. Wayne[f], E. Won[i], Y. Yu[j]

[a]Fermi National Accelerator Laboratory, [b]University of Illinois at Chicago, [c]Korea University, [d]Kyungsung University, [e]Northeastern University, [f]University of Notre Dame, [g]Purdue University, [h]Rice University, [i]University of Rochester, [j]Seoul National University

Abstract

A large scale scintillating fiber tracker using visible light photon counter (VLPC) readout was built as a prototype for the upgraded DØ central tracker. This prototype has been under test at Fermilab for six months using cosmic rays. A description of the components of the tracker including the photodetector, fibers, lightguides, ribbons, and DAQ is given. Preliminary results on detected photon yield, position resolution, efficiency and VLPC performance are presented.

I. INTRODUCTION

The DØ Detector [1] at Fermilab is used to study proton-antiproton collisions at a center of mass energy of 1.8 TeV. Evolution of the physics goals of the DØ Collaboration, as well as increasing Tevatron luminosity, necessitates an upgrade of the DØ Detector [2]. The main thrust of this upgrade will be a new central detector. Proceeding outwards in radius it consists of a microstrip silicon tracker composed of a combination of 4 barrels and 16 disks; a four superlayer scintillating fiber outer tracker with two stereo and two r-ϕ measurements per superlayer; a 2 Tesla superconducting solenoid; and a six layer preshower detector with two axial and four stereo layers.

This paper describes the construction and the results of the study of the prototype of the scintillating fiber outer tracker. While systems using small numbers (<128) of scintillating fibers with VLPC readout have been studied previously in order to develop proof-of-principle of the fiber tracking technique [3,4], here we report on a system-level study of 3072 fiber/VLPC channels.

II. DETECTOR COMPONENTS

A. Setup

A schematic layout of the cosmic ray test stand is shown in Fig. 1. The main components are three superlayers of scintillating fibers each with four doublets in x:u:v:x configuration, where x is shorthand for layers with fibers parallel to the axis of the cylinder, and u and v are at $\pm 2^{o}$ with respect to x. Two superlayers are mounted on a carbon fiber cylinder and the third on a flat carbon fiber board inside it. There are 3072 scintillating fibers arranged into 24 singlet layers, 128 fibers wide. Scintillation counters provide a cosmic ray trigger with 0.8 GeV/c and 2.5 GeV/c thresholds set by the amount of traversed steel. There are also three planes of Iarocci tubes, providing additional tracking capabilities.

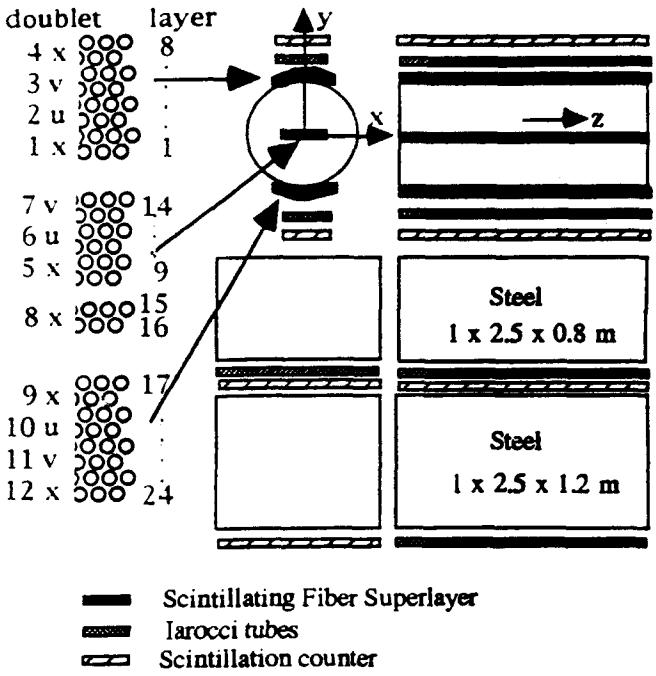

Fig. 1. Cosmic ray test stand (see text for details).

B. Single Detector Element

A single element of the tracker is shown schematically in Fig. 2. An ionizing particle produces light in a scintillating fiber. Trigger counters limit particle trajectories to the 2 m long central portion of the 2.8 m long scintillating fiber. One end of the fiber is covered by an aluminized mylar mirror that reflects light towards the photodetector. The light propagates through an optical connector, an 8.0 m clear fiber, another connector, a 50 cm clear fiber located inside a cryogenic container (called a "cassette") and finally reaches a VLPC photosensor maintained at a temperature of about 6.5 K. The output signal from the VLPC is transmitted via Teflon coated stainless steel strip cable to a QPA02 preamplifier [5] located

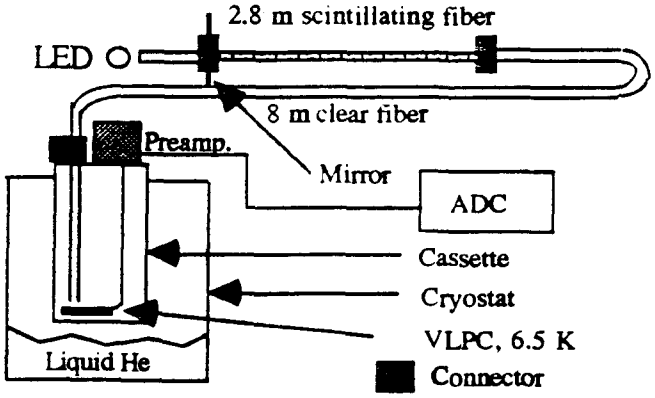

Fig.2. Schematic view of single detector element.

at the room temperature end of the cassette. The QPA02 has a differential impulse gain of 17 mV/fC. The analog signal from the preamplifier is digitized by FASTBUS ADCs. For calibration, each element can also be illuminated by an LED coupled through a light guide and an optical connector to the non-readout end of the scintillating fiber [6]. LED light is injected through the aluminized mylor mirror.

C. Photodetectors

Light is detected by Visible Light Photon Counters (VLPC), derivatives of the solid state photomultiplier developed by the Rockwell International Science Center [7]. VLPCs were chosen because of their high quantum efficiency (> 60 %), high gain (> 15000), low gain dispersion of 15 %, an intrinsic time resolution equal to or better than 100 ps, and low noise of < 10 kHz at 0.5 photoelectron threshold. In the summer of 1993 a total of about 5000 VLPC pixels, designated HISTE IV, were delivered to Fermilab as bare die in arrays of 8 pixels of 1 mm diameter on 1.05 mm pitch. A "hybrid" was formed by mounting an 8 pixel VLPC array on a aluminum-nitride substrate with the output pads of pixels wire-bonded to the output traces on the substrate. All hybrids were characterized in a special test cassette. The devices were then ranked according to the number of non-functional channels due either to high noise or lack of response, and the best hybrids were used in the tracker. The gain and the relative quantum efficiency were determined for all devices.

D. Fibers and Ribbons

Multiclad scintillating fibers of 835 μm diameter, fabricated by Kuraray Corporation, were chosen because of their high light yield and excellent attenuation length. The core of these fibers, emitting light at a peak wavelength of λ_p = 525 nm, consists of polystyrene doped with 1 % by weight of p-terphenyl and 1500 ppm of 3-hydroxyflavone (3HF). Polystyrene has a refractive index of 1.59. It is surrounded by inner (PMMA) and outer (flouro-acrylic) claddings having refractive indices of 1.49 and 1.42. The multiclad fibers provide a factor of 1.4 to 1.8 larger light yield than single clad fibers [4] because of the increase of the numerical aperture due to the lower refractive index of the outermost cladding. The clear waveguide fibers are of an identical multiclad construction but with a 965 μm diameter.

Singlet ribbon layers of 128 scintillating fibers with 870 μm center to center spacing were formed by laying fibers into grooved jig-plates. The spacings of the grooves were precise to 10 μm over a 2 m length. Next, a thin Kapton tape was placed over the fibers securing them into a singlet layer. Doublet ribbon layers were formed by gluing two singlet layers together while maintaining an offset of a half fiber spacing between the singlets. Each singlet was terminated with a 128-hole connector made of Delrin plastic. The fibers were inserted into a connector and then potted with an optical epoxy. The face of the potted fiber and connector assembly was then finished with a diamond fly cutting machine. Clear light guide fibers were arranged into bundles of 128 fibers each and were terminated with matching connectors. The light transmission through mated connectors was measured to be 95 %.

Under a large Coordinate Measuring Machine (CMM) the doublet ribbons were then mounted on the carbon fiber support cylinder of 27 cm radius and 200 cm length. Doublets were aligned with the cylinder axis (or set at an angle for stereo) and then were mounted with contact adhesive. Fiber positions were measured by multiple probe touches of the CMM.

E. Cassettes and Cryogenics

The VLPC cassettes each hold 128 channels (16 x 8 pixel arrays) of HISTE IV devices. Each singlet fiber ribbon layer (128 fibers) was mapped into a single cassette. The hybrids were mounted on a carbon-loaded plastic (Torlon) holder that has holes into which clear 50 cm long fibers were threaded and aligned with the pixels. The alignment was done optically to a precision of 10 μm. The cassette has temperature monitoring resistors and a heater resistor that allow for precise temperature control using an external temperature controller. A single cryostat houses all 24 cassettes in the system and cools all 3072 pixels. Liquid He supplied from a 10,000 liter dewar is transferred into the cryostat via a vacuum insulated transfer line. Cooling of the VLPCs is done convectively through a separate gaseous He volume that is in direct contact with a copper isotherm operated at liquid He temperature.

F. Data Taking

Analog signals from all 3072 scintillating fibers as well as from the Iarrocci tubes are fed to FASTBUS 1885N LeCroy ADC's where they are integrated for 100 ns and digitized with a sensitivity of 0.05 pC per count. Data are written out to exabyte tapes for off-line analysis. A coincidence of three or four scintillation counters provides a cosmic ray trigger of 2Hz at a 0.8 GeV/c threshold or 0.5 Hz at a 2.5 GeV/c threshold. Data taken with the cosmic ray trigger are used for tracking analysis. Two other triggers are also utilized: a pulser trigger providing a noise measurement; and a trigger activating LEDs and thus enabling a determination of the gain of the VLPCs.

Data were taken with VLPCs at a temperature of 6.5 K, a temperature at which the VLPC is fully efficient. A study was done to determine the optimum bias voltage. In this study, the efficiency of fibers. was computed as a function of the bias voltage while the threshold was set to keep the noise rate constant. The efficiency varies slowly within the studied range

of 6.2 V to 7.0 V, with the maximum efficiency at 6.5 V. Most of the data were taken at this optimum bias voltage over a period of a half year with the goal to study performance and long term stability of the system.

III. RESULTS

A. Tracking

The first step in track reconstruction is the formation in the fiber singlet layers of coordinate clusters which are contiguous sets of fibers with pulse heights exceeding 6σ of the pedestal distribution (at 6.5 V bias voltage this corresponds to a 1.5 photoelectron threshold). The spatial coordinate assigned to each cluster is the centroid position of the fiber with the largest pulse height. The majority of clusters contain one fiber only.

Track finding is initiated using the axial fiber layers. At least two single layers in each superlayer and seven or more layers in total are required to have clusters, and straight lines are fitted to all possible combinations of the clusters. Clusters deviating more than 0.75 times the fiber spacing from the line are removed and the remaining clusters are fitted to a straight line again. This process is repeated until all clusters are within the allowed tolerance or the number of layers which participate in the fit has reached two for each superlayer or seven in total. Finally a χ^2 cut to the overall track is then applied.

Stereo layers are used to fit the track in the z-y view (y is the vertical axis and z is along the axis of a cylinder; see also Fig. 1). Given the x of the track, z coordinates associated with clusters in each stereo layer are calculated and then these positions are used to fit a straight line in the z-y view in a manor analogous to the axial view. The slopes Δx/Δy, Δz/Δy and the z distribution of the fitted tracks are presented in Fig. 3.

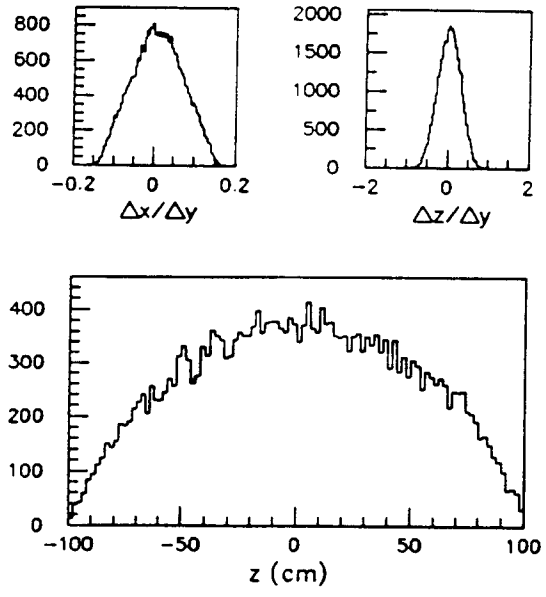

Fig. 3. Slope and z distribution of the tracks in layer # 9.

B. Doublet Resolution

The position resolution of a fiber doublet was measured as follows. Clusters from two outer axial doublets are connected by a straight line and the residuals of the clusters from a third axial doublet are plotted. A typical distribution is shown in Fig. 4. The width of this distribution is $\sqrt{3/2}$ times the actual doublet resolution because of the error in position on the outer two clusters. The position resolution of a fiber doublet in the r-φ view is σ_x = (136.2 ± 0.6) μm for tracks with a momentum cut-off of 2.5 GeV/c. The z coordinate resolution, determined in a similar way, is σ_z = (4.17 ± 0.04) mm. This is consistent with $\sigma_z/\sigma_x = 30$, as expected from the 2^0 stereo angle.

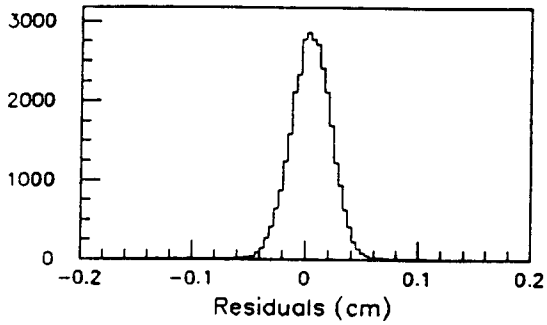

Fig. 4. Distribution of residuals in r- φ view.

C. Photoelectron Yield

To measure the average number of photoelectrons from fibers in a singlet fiber layer, the tracks are reconstructed without the doublet containing that singlet layer. The fit tracks are then extrapolated to that layer. The pulse height of fibers whose centers are within 350 μm distance of the fit line are plotted. The pulse height distribution obtained in such a way for axial singlet layer # 9 is shown in Fig. 5. The average

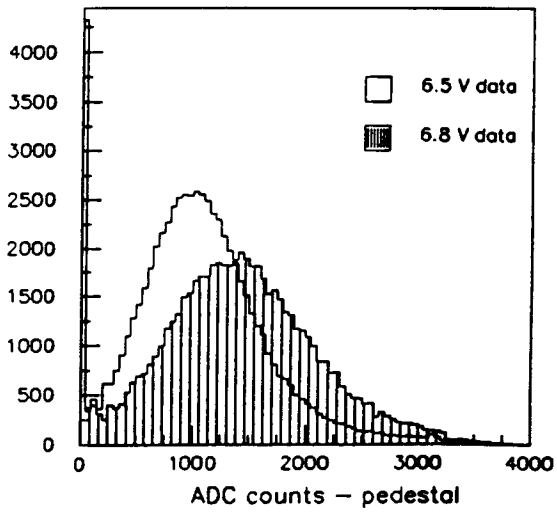

Fig. 5. Pulse height spectra of hit fibers at 6.5 V and 6.8 V bias voltage.

number of detected photoelectrons for a given bias was obtained from Fig. 5 by dividing the average pulse height at that bias by the appropriate gain. The gain at 6.5 V and 6.8 V bias is 109.4 and 139.5 ADC counts per photoelectron (see section E). The average number of photoelectrons detected at the bias voltages of 6.5 V and 6.8 V is 9.6 and 10.0, respectively.

Another measure of the photoelectron yield is the most probable pulse height after exclusion of the peak at zero pulse height. Gaussian fits were made around the most probable pulse height, and the means for the axial layers are plotted in Fig. 6. For example in layer # 9 the most probable pulse height is equal to 9.1 photoelectrons, 0.5 photoelectron less than the average of the total pulse height distribution.

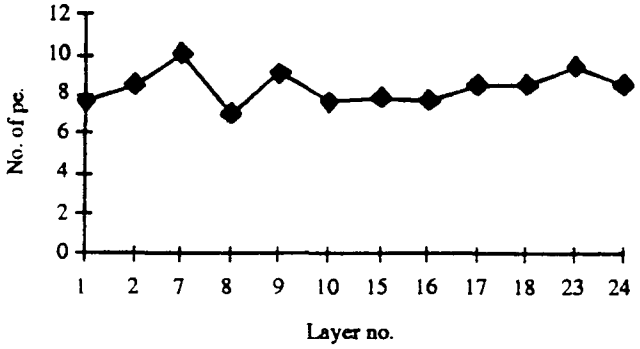

Fig. 6. Most probable pulse height for axial layers.

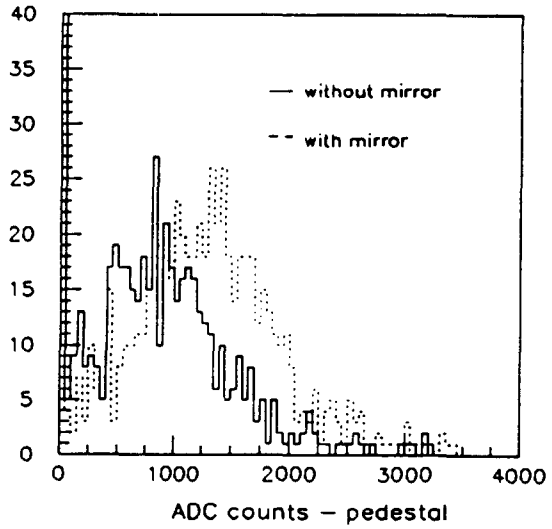

Fig. 7. Pulse height spectra with and without mirrors.

The data were also taken with mirrors removed from the ends of the fibers. The pulse height spectra with and without mirrors are compared in Fig. 7 and the respective mean values are 1213 and 881 ADC counts. Here mirroring is found to increase the photoelectron yield by 38 % , corresponding to a reflectivity of 0.64.

D. Efficiency

The efficiency of the singlet layer was determined by studying the pulse height in the fibers of a doublet layer that was not used to define a track. The track is extrapolated into that layer and if both fibers closest to the track are functional channels the event is kept. Efficiency is found by checking if either of these fibers has a signal above a threshold. The threshold is chosen in order to keep noise below a certain value. At a threshold corresponding to a noise rate of 0.1 %, typical single layer efficiency was found to be 85 % which is essentially the geometric efficiency of a singlet layer.

Table 1. Efficiency of doublet # 8 at various thresholds.

Noise level (in %)	Efficiency including noise	Efficiency after noise subtraction
0.025	0.9988±0.0001	0.9960±0.0002
0.050	0.9990±0.0001	0.9953±0.0002
0.075	0.9991±0.0001	0.9944±0.0003
0.100	0.9992±0.0001	0.9933±0.0003
0.125	0.9992±0.0001	0.9925±0.0003

The efficiency of the doublet was measured similarly. The four fibers closest to the extrapolated track are checked for the pulse height above various thresholds. The efficiencies after noise subtraction for the doublet # 8 are presented in Table 1. They are almost 100 % regardless of the threshold.

E. Gain , noise and stability of HISTE IV devices

Gain and gain dispersion were determined by illuminating fibers with LED light. By adjusting the voltage on the LED's, the amount of light emitted by LED's was such that only a few photoelectrons were generated in the VLPC's. A typical pulse height spectrum thus obtained is shown in Fig. 8. The gain for every pixel was defined as the difference, in ADC counts, between the first photoelectron peak and the pedestal. These gains for all channels are plotted in Fig. 9. The RMS of the gain spread at 6.5 V bias is 9%, which is an upper limit since the variations from channel to channel in amplifier gain and ADC conversion are not taken out. Next, for every pixel the ratio of the gain measured in October 1994 to the gain measured in May 1994 was calculated. These measurements

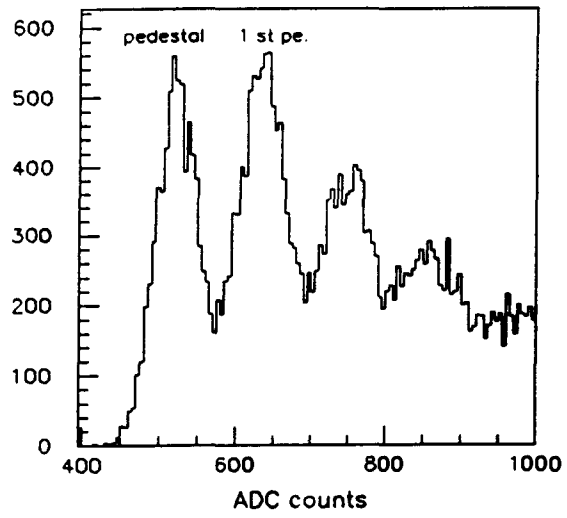

Fig. 8. Pulse height spectrum in one of the pixels illuminated with LED light.

are plotted in Fig. 10. The mean value is 0.995 with an RMS of 5%, implying good stability of the gain over the six month period of study.

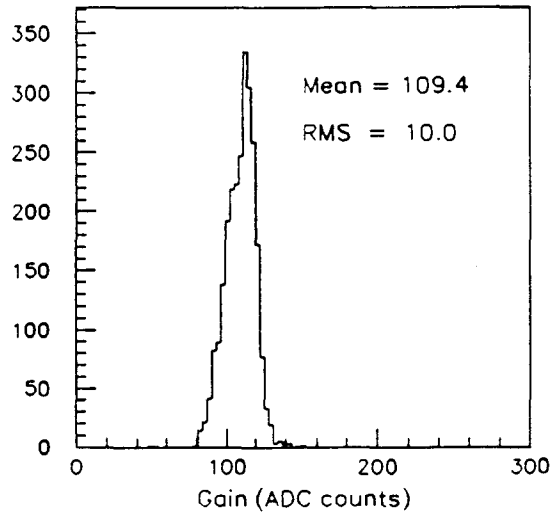

Fig. 9. Gain distribution at the bias voltage of 6.5 V.

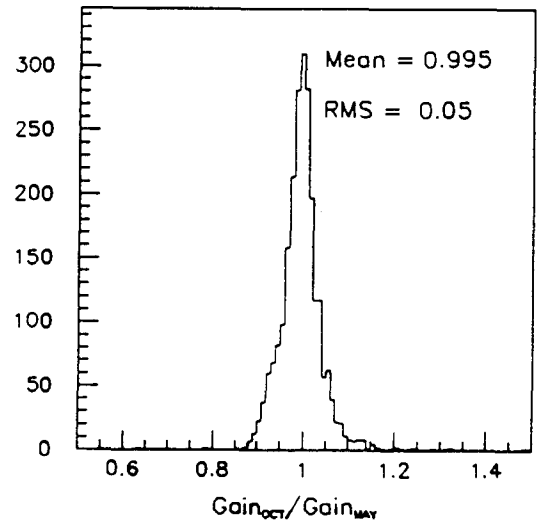

Fig. 10. The ratio of the gain measured in October 1994 to the gain measured in May 1994.

The gain dispersion was determined by comparing the width of the first photoelectron peak to the width of pedestal peak (Fig. 11). The total width of the first photoelectron peak is assumed to be the sum, in quadrature, of the pedestal width and the VLPC gain dispersion. The average gain dispersion for all pixels in May 1994 and Oct. 1994 was 14.7 %. Table 2 summarizes these results.

Noise rates were determined from data taken with a pulser trigger by counting the rates above various thresholds. In Fig. 12 we present the distribution of thresholds for all channels for a noise level of 0.1 % at a bias voltage of 6.5 V. On average, we need a threshold of 0.94 photoelectrons to set the noise at the level of 0.1 %. The dependence of the average threshold on the noise rate is presented in Fig. 13 for two measurements, one in May 1994 and another one in October 1994. The noise rates remained constant over the period of study.

Table 2. Average σ pedestal and σ of 1st pe. in ADC counts and σ of gain dispersion in %.

	σ of pedestal	σ of 1 st pe.	σ of gain dispersion
May 94	27.4	32.3	14.7
Oct. 94	27.0	31.9	14.7

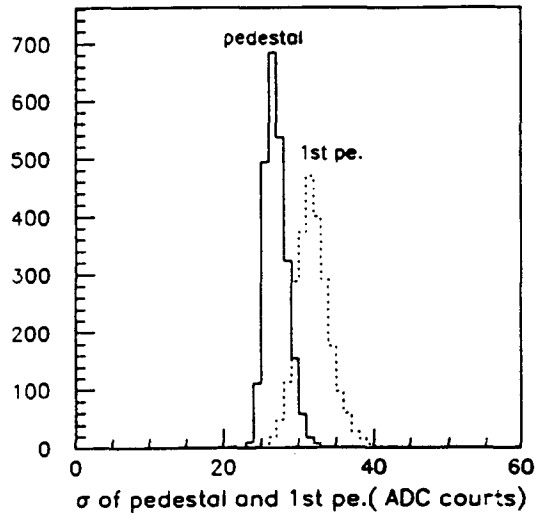

Fig. 11. The distribution of the widths of the pedestal and of the first photoelectron peak.

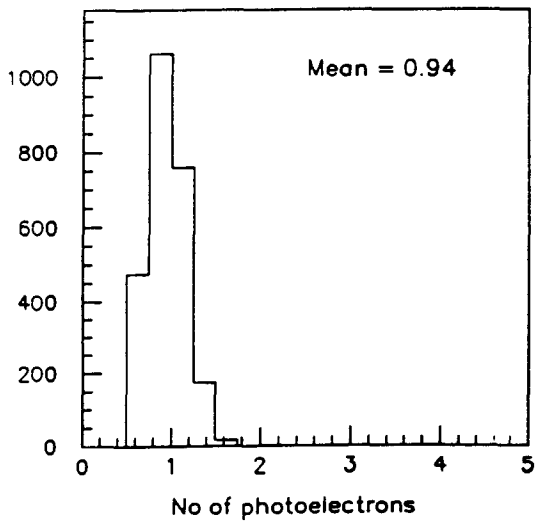

Fig. 12. The distribution of thresholds for a noise level of 0.1 %.

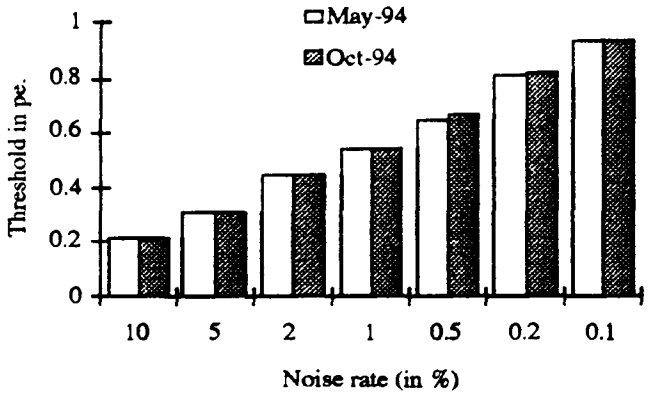

Fig. 13. Thresholds in photoelectrons as a function of noise rate.

IV. CONCLUSIONS

A system level test of 3072 scintillating fiber/VLPC channels has been carried out. The system utilized scintillating fibers of 835 μm diameter and 2.8 m length, coupled to clear fiber waveguides of 965 μm diameter and 8 m length. All fibers were of multiclad construction. Readout was via HISTE IV VLPCs.

We have observed the following. The most probable number of photoelectrons averaged over axial singlet layers is 8.4 photolectrons at 6.5 V bias voltage. The spatial resolution of a doublet in the axial view was found to be (136.2 ± 0.6) μm. After correcting for the non-functional channels, the efficiency of a doublet was determined to be higher than 99%. VLPC gain, gain dispersion, and noise were demonstrated to be constant over the period of study. These measurements indicate that the scintillating fiber detector proposed for the DØ upgrade will be an efficient, high precision tracking system.

V. ACKNOWLEDGMENTS

We thank the support staffs at each of the participating institutions. The technical staff within the Research and Computing Divisions and the Physics and Technical Sections at Fermilab have played vital roles in the design, fabrication, and operation of this system. Financial support has been provided by the U.S. Department of Energy, the U.S. National Science Foundation, Korean Ministry of Education, Korean Research Foundation and KOSEF in Korea.

VI. REFERENCES

1. S. Abachi et al., Nucl. Instr. and Meth. A 338 (1994) 185.
2. S. Grünendahl in Proceedings of 9th Topical Workshop on Proton- Antiproton Collider Physics, ed. K .Kondo and S. Kim (Universal Academy Press, Inc., 1994), p. 374.
3. M. Atac et al., Nucl. Instr. and Meth. A 320 (1992) 155.
4. B. Baumbaugh et al., Nucl. Instr. and Meth. A 345 (1994) 271 and references cited within.
5. T. Zimmerman, IEEE Trans. on Nucl. Sci. 37 (1990) 439.
6. B. Baumbaugh et al., these proceedings.
7. M. D. Petroff et al., Appl. Phys. Lett. 51 (1987) 406.